H2AEOLUS

DELIVERABLE D6.2

Control system for energy-storage use case

PUBLIC

M. B. Abdelghany, M. F. Shehzad,
V. Mariani, D. Liuzza, L. Glielmo (UniSannio)
Quality Assurance: F. Zenith (SINTEF)

Project acronym:	HAEOLUS
Project title:	Hydrogen-Aeolic Energy with Optimised eLectrolysers Upstream of Substation
Project number:	779469
Call:	H2020-JTI-FCH-2017-1
Topic:	FCH-02-4-2017
Document date:	December 12, 2019
Due date:	May 31, 2019
Keywords:	Energy storage systems, hydrogen conversion, power to gas, energy management, model predictive control, mixed logic dynamics, power smoothing

Abstract: The current deliverable regards the formulation of a Model Predictive Control (MPC) policy for hydrogen based storage plants in the energy-storage use case to be implemented within the EU-FCH 2 JU (European Union Fuel Cells and Hydrogen 2 Joint Undertaking) funded project HAEOLUS.
The proposed policy relies in part upon the analysis and the modeling already presented in the previous deliverable and adapt them to the new use case. The novel dynamic model of the hydrogen based storage plant developed in this deliverable is a five states automaton for both the electrolyzer and the fuel cell. The motivation for such study are to simultaneously smooth the real wind power output and optimize the storage performance of the energy storage system (ESS) while tracking the grid operator reference. These two different (and possibly conflicting) goals pose a two objective optimization problem, by giving priority first to the output power smoothing and then to the tracking of the grid operator reference. The overall system is subject to hard constraints in terms of energy storage system requirements, ramp rate requirements, feasible operational modes and corresponding transitions. Specifically, since the smoothing problem is significant for short time scales, a detailed model of the hydrogen storage system has been derived to well capture the equipments behaviour.

Revision History

Date	Description	Author (organisation)
2019/Jul/2	First draft	Valerio Mariani (UniSannio)
2019/Jul/2	Add Abstract, Introduction, System description and MPC controller architecture	Valerio Mariani (UniSannio)
2019/Jul/17	Add System modeling (in progress)	Valerio Mariani (UniSannio)
2019/Jul/18	Add System modeling and Conclusions (in progress)	Valerio Mariani (UniSannio)
2019/Jul/18	Add System modeling and Conclusions	Valerio Mariani (UniSannio)
2019/Jul/22	Review text for issues and inconsistencies fixing before Davide's doublecheck	Valerio Mariani (UniSannio)
2019/Jul/22	Review text for issues and inconsistencies fixing	Valerio Mariani (UniSannio)
2019/Jul/30	Review text for issues and inconsistencies fixing	Valerio Mariani (UniSannio)
2019/Oct/15	Review text for issues and inconsistencies fixing	Valerio Mariani (UniSannio)
2019/Nov/15	Review text for issues and inconsistencies fixing	Valerio Mariani (UniSannio)
2019/Dec/6	Review text for issues and inconsistencies fixing	Valerio Mariani (UniSannio)
2019/Dec/10	Review text for issues and inconsistencies fixing	Valerio Mariani (UniSannio)

This project has received funding from the Fuel Cells and Hydrogen 2 Joint Undertaking under the European Union's Horizon 2020 research and innovation programme under grant agreement № 779469.

Any contents herein reflect solely the authors' view. The FCH 2 JU and the European Commission are not responsible for any use that may be made of the information herein contained.

Table of Contents

1 Introduction

This deliverable reports the advancements regarding the high-level control algorithms for the integrated wind-hydrogen system developed under the EU-FCH JU project HAEOLUS – Hydrogen-Aeolic Energy with Optimized eLectrolyzers Upstream of Substation [1].

Specifically, in this deliverable the control algorithms regarding the wind-hydrogen system operated within the energy-storage use case are presented. In the energy-storage use case the purpose is to balance short-term fluctuations in wind power, producing hydrogen at times of surplus power production and re-electrifying it during periods of underproduction, thus easing wind power integration at large scale, independently of support from fossil-fuel power stations [2, 3]. In addition to power smoothing, in order to present a general control architecture which will be kept also for the development of further services, the grid operator reference tracking is addressed as well.

The developed control algorithm takes advantage of the hydrogen-based Energy Storage System (ESS). Standard techniques tackle the problem by introducing suitable passive filters in order to smooth the power from a wind farm. In an eco-friendly perspective, to dissipate power may look contradictory even with the aim of meeting power quality requirements, while active strategies can provide a nice mean to preserve grid operations and efficiency at the same time.

2 Nomenclature

The parameters, the forecasts, and the decision variables used in the proposed formulation are described, respectively, in Table 1, Table 2 and Table 3.

3 System Description

A system block diagram is shown in Figure 1. The wind power flow, the hydrogen flow and the data flow are denoted by green, blue and red lines, respectively. Accordingly, P_w indicates the power generated by the wind farm, $P_{\mathrm{e}}^{\mathrm{ON}}$ indicates the input power of the electrolyzer, $P_{\mathrm{f}}^{\mathrm{ON}}$ indicates the output power of the fuel cell, P_{dump} is the power that can be dissipated by a resistive load when needed and P_{ref} is the reference signal from the grid operator which has to be tracked by P_{avl}.

In an ideal condition, where P_w matches exactly the grid operator reference, the hydrogen based ESS is not operated. However, in a real condition, the excess power from the wind turbines is used to produce hydrogen through electrolysis, then the generated hydrogen is stored in a hydrogen tank and re-electrified by the fuel cell in low or nearly zero wind production.

4 System Modeling

We utilize a framework for modeling and controlling the hydrogen storage system, consisting of interdependent physical laws, logical rules, and operating constraints, denoted as mixed logical dynamical (MLD) systems. MLD models are suitable for solving problems combining binary

Table 1: List of parameters.

Parameters	Description	Units
$H^{\max}$	Maximum Level of the hydrogen storage unit	kg
$H^{\min}$	Minimum Level of the hydrogen storage unit	kg
$P_{\mathrm{e}}^{\max}$	Maximum power level of the electrolyzer	kW
$P_{\mathrm{e}}^{\min}$	Minimum power level of the electrolyzer	kW
$P_{\mathrm{e}}^{\mathrm{CLD}}$	Power required by the electrolyzer for cold starts	kW
$P_{\mathrm{e}}^{\mathrm{STB}}$	Power required by the electrolyzer in stand-by	kW
$P_{\mathrm{e}}^{\mathrm{WRM}}$	Power required by the electrolyzer for warm starts	kW
$P_{\mathrm{f}}^{\max}$	Maximum power level of fuel cell	kW
$P_{\mathrm{f}}^{\min}$	Minimum power level of fuel cell	kW
$P_{\mathrm{f}}^{\mathrm{CLD}}$	Power required by the fuel cell for cold starts	kW
$P_{\mathrm{f}}^{\mathrm{STB}}$	Power required by the fuel cell in stand-by	kW
$P_{\mathrm{f}}^{\mathrm{WRM}}$	Power required by the fuel cell for warm starts	kW
$\mathrm{NH_e}$	Number of life hours of the electrolyzer	h
$\mathrm{NH_f}$	Number of life hours of the fuel cell	h
$\mathrm{HY_f}$	Number of per year life hours of the fuel cell	h
$\mathrm{HY_e}$	Number of per year life hours of the electrolyzer	h
$\mathrm{HY_f}$	Number of per year life hours of the fuel cell	h
η_e	efficiency of the electrolyzer production rate	kg/Wh
η_f	efficiency of the fuel cell consumption rate	Wh/kg
$\mathrm{R_e}$	Ramp limit of the electrolyzer	kW/s
$\mathrm{R_f}$	Ramp limit of the fuel cell	kW/s
$S_{\mathrm{rep,e}}$	Electrolyzer stack replacement cost	€/kW
$S_{\mathrm{rep,f}}$	Fuel cell stack replacement cost	€/kW
T_s	Sampling period	h
T	Simulation horizon	h

Table 2: Forecasted powers.

Forecasts	Description
P_w	Wind power production kW
P_{ref}	Grid operator reference kW

Table 3: Real and logical time varying variables.

Variables	Description
$\sigma_{\alpha_e}^{\beta}$	State transitions of the electrolyzer $\alpha, \beta \in \{\text{OFF}, \text{CLD}, \text{STB}, \text{WRM}, \text{ON}\}$
$\sigma_{\alpha_f}^{\beta}$	State transitions of the fuel cell $\alpha, \beta \in \{\text{OFF}, \text{CLD}, \text{STB}, \text{WRM}, \text{ON}\}$
z_i^{γ}	Electric power formulated as mixed logic dynamic (MLD) variable $\gamma \in \{\geq 0, \leq 0, \geq P_i^{\text{CLD}}, \leq P_i^{\text{CLD}}, \geq P_i^{\text{STB}}, \leq P_i^{\text{STB}}, \geq P_i^{\text{WRM}}, \leq P_i^{\text{WRM}}, \geq P_i^{\min}, \leq P_i^{\max}\}$
δ_e^{ON}	Logical variable corresponding to on mode of the electrolyzer
δ_e^{OFF}	Logical variable corresponding to off mode of the electrolyzer
δ_e^{STB}	Logical variable corresponding to standby mode of the electrolyzer
δ_e^{CLD}	Logical variable corresponding to cold mode of the electrolyzer
δ_e^{WRM}	Logical variable corresponding to warm up mode of the electrolyzer
δ_f^{ON}	Logical variable corresponding to on mode of the fuel cell
δ_f^{OFF}	Logical variable corresponding to off mode of the fuel cell
δ_f^{STB}	Logical variable corresponding to standby mode of the fuel cell
δ_f^{CLD}	Logical variable corresponding to cold mode of the fuel cell
δ_f^{WRM}	Logical variable corresponding to warm up mode of the fuel cell
P_{avl}	Available power delivered to the grid kW
H	Stored level of the hydrogen kg

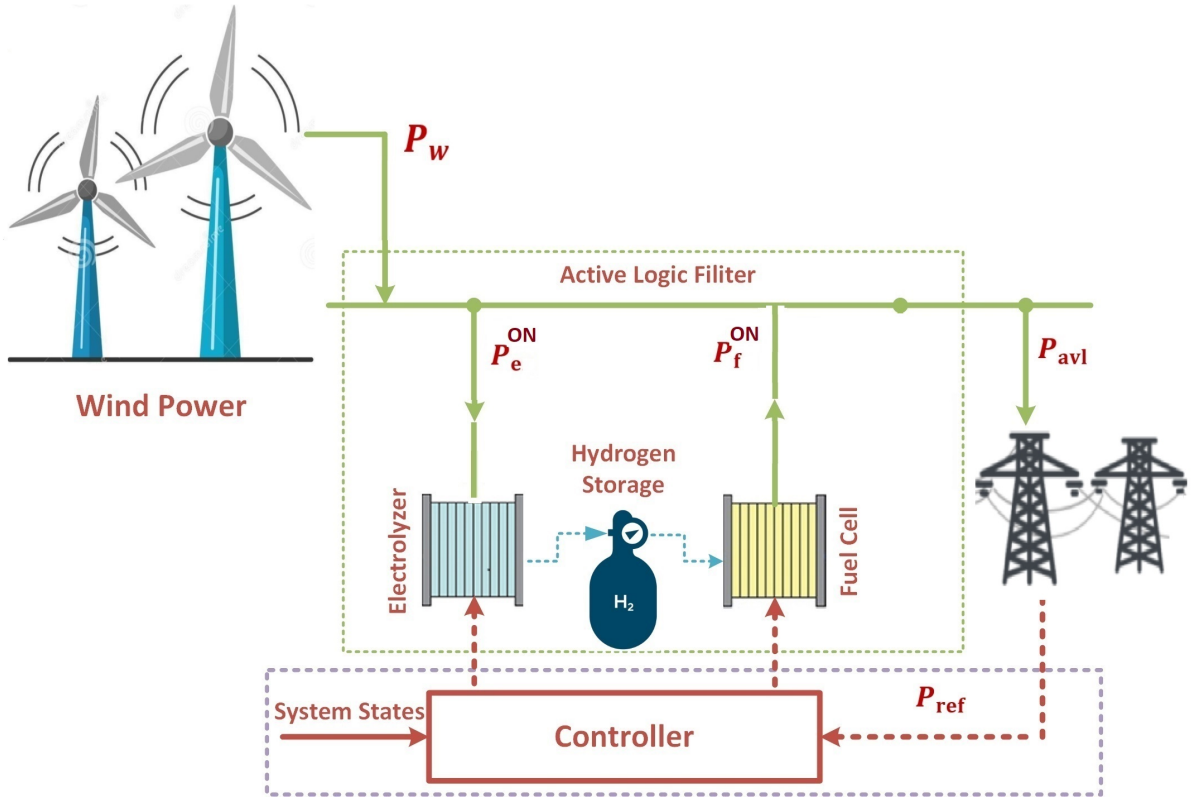

Figure 1: HAEOLUS' hydrogen based storage system modeled in this deliverable. $P_{\mathrm{e}}^{\mathrm{ON}}$, $P_{\mathrm{f}}^{\mathrm{ON}}$, and P_w are the electrolyzer input power, the fuel cell output power and the wind power, respectively. Also, P_{ref} is the grid operator reference which has to be tracked by P_{avl}.

variables and continuous variables with the help of definition given in Bemporad et al. [4]. Based on the derived MLD framework, the model can be realized optimally via mixed integer programming (MIP) algorithm.

All the equations are derived in a discrete time fashion. We denote with k the discrete time. The (physical) continuous time t can be immediately obtained via $t = kTs$, with Ts being the sampling time. In this deliverable, the sampling time is supposed to be of one hour and all the parameters in the equations are computed according to it.

Since, the devices can be operated in 3 different physical modes, namely the on mode, the off mode and the stand-by mode, we will consider two corresponding automaton each one including the states ON, OFF and STB, as shown in Figure 2. However, the additional CLD and WRM states are added in order to account for cold and warm starts within the corresponding cost functions. Modeling of cold and warm states gives the proposed controller extra degrees of freedom to find an optimal solution by putting the devices either in stand-by mode or in off considering the fact that a faster response can be achieved in stand-by state with a trade-off of providing a constant 1kW of power to keep their stacks warm even though in this state their production/consumption is null. On the other hand, in off mode the devices has to meet the exact amount of long waiting time constraint in order to go again into their production or consumption states [1].

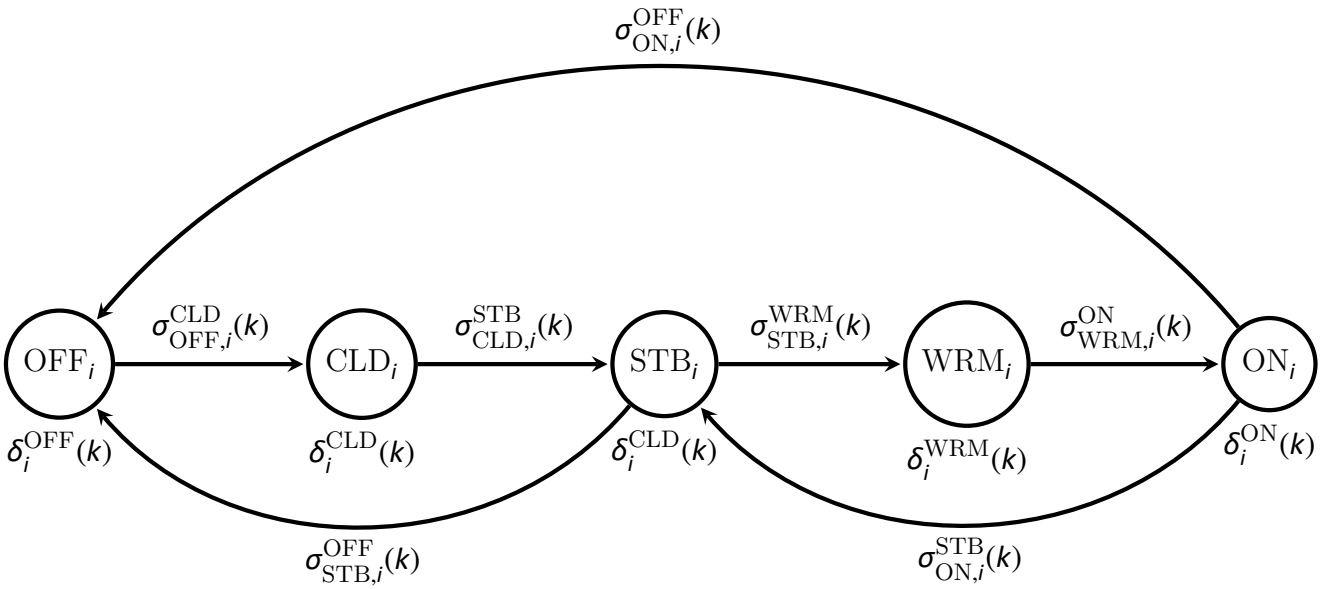

Figure 2: Automaton for the electrolyzer ($i = e$) and the fuel cell ($i = f$).

4.1 Discrete Operational States of the Electrolyzer and the Fuel cell

The discrete operational states of the devices are presented in this section. As shown by the graph in Figure 2, each node represents a particular state (i.e. operational mode) and the edges represent transitions among states. Both the states and the edges are labeled with corresponding mutually exclusive binary variables $\delta_i^{\alpha}(k)$ and $\sigma_{\alpha,i}^{\beta}(k)$, respectively, with $\alpha, \beta \in \{\mathrm{OFF}, \mathrm{CLD}, \mathrm{STB}, \mathrm{WRM}, \mathrm{ON}\}$ and $i \in \{e, f\}$. The operational states and switching of the devices have been modeled and discussed in the two following subsections.

4.1.1 Mathematical Model and MLD Constraints Formulation of the States

The five discrete states OFF, CLD, STB, WRM and ON of the each automaton are identified by the product of one logical variable and one power, which is relevant for that state, to be different from zero. For instance, whenever the electrolyzer is in the ON state, the corresponding input power is limited within the range $[P_e^{\min}, P_e^{\max}]$. Thus, by defining $P_e(k)\delta_e^{\mathrm{ON}}(k) = P_e^{\mathrm{in}}$ and since in this case we set $\delta_e^{\mathrm{ON}} = 1$ then it results also $P_e(k) = P_e^{\mathrm{in}} \in [P_e^{\min}, P_e^{\max}]$. Moreover, being by definition mutually exclusive for each $i \in \{e, f\}$, all other logical variables δ_e^{α}, $\alpha \neq \mathrm{ON}$ are null, instead. On the other hand, whenever the electrolyzer is in the STB state, the relevant power to be considered is the stand-by power P_e^{STB}. Therefore, by defining $P_e(k)\delta_e^{\mathrm{STB}}(k) = P_e^{STB}$ it follows that $P_e(k) = P_e^{STB}$ since accordingly $\delta_e^{\mathrm{STB}}(k) = 1$, while, again, all other logical variables δ_e^{α}, $\alpha \neq \mathrm{STB}$ are null. Similar considerations apply in case of the WRM and the CLD states. Finally, when the electrolyzer is in the OFF state, its corresponding input power along with the power consumption are null, resulting in $P_e(k) = 0$.

In general, the meaning of $P_i(k)$ depends on the condition of the i-th device that, in turn, is identified by the corresponding $\delta_i^{\alpha}(k)$. That is, $P_i^{\alpha} = P_i\delta_i^{\alpha}(k)$, and therefore, according to the op-

erating condition of the i-th device, each $\delta_i^{\alpha}(k)$ with $i \in \{e, f\}$ and $\alpha \in \{\mathrm{OFF}, \mathrm{CLD}, \mathrm{STB}, \mathrm{WRM}, \mathrm{ON}\}$ is determined as

$$\begin{cases} P_i^{\min} \leq P_i(k) \leq P_i^{\max} & \iff \delta_i^{\mathrm{ON}} = 1, \\ P_i(k) = P_i^{\mathrm{CLD}} & \iff \delta_i^{\mathrm{CLD}} = 1, \\ P_i(k) = P_i^{\mathrm{STB}} & \iff \delta_i^{\mathrm{STB}} = 1, \\ P_i(k) = P_i^{\mathrm{WRM}} & \iff \delta_i^{\mathrm{WRM}} = 1, \\ P_i(k) = 0 & \iff \delta_i^{\mathrm{OFF}} = 1. \end{cases} \tag{1}$$

In order to cope with an optimal control framework, the cases above (the if-then-else conditions as in (1)) need further manipulations to derive MILP constraints (we refer the interested reader to [4] for guiding details). For this reason, as an intermediate step, we introduce auxiliary Boolean variables defined as

$$z_i^{\gamma^{\geq}}(k) = \begin{cases} 1 & P_i(k) \geq \bar{\gamma}^{\geq}, \\ 0 & P_i(k) < \bar{\gamma}^{\geq}, \end{cases} \tag{2a}$$

$$z_i^{\gamma^{\leq}}(k) = \begin{cases} 0 & P_i(k) > \bar{\gamma}^{\leq}, \\ 1 & P_i(k) \leq \bar{\gamma}^{\leq}, \end{cases} \tag{2b}$$

with $i \in \{\mathrm{e}, \mathrm{f}\}$, $(\gamma^{\geq}, \gamma^{\leq}) \in \{(\geq 0, \leq 0), (\geq P_i^{\mathrm{CLD}}, \leq P_i^{\mathrm{CLD}}), (\geq P_i^{\mathrm{STB}}, \leq P_i^{\mathrm{STB}}), (\geq P_i^{\mathrm{WRD}}, \leq P_i^{\mathrm{WRD}}), (\geq P_i^{\min}, \leq P_i^{\max})\}$ and $(\bar{\gamma}^{\geq}, \bar{\gamma}^{\leq}) \in \{(0,0), (P_i^{\mathrm{CLD}}, P_i^{\mathrm{CLD}}), (P_i^{\mathrm{STB}}, P_i^{\mathrm{STB}}), (P_i^{\mathrm{WRM}}, P_i^{\mathrm{WRM}}), (P_i^{\min}, \geq P_i^{\max})\}$. By using the transformations defined in [4], the above formulas can be expressed with the following compact inequalities for each cases:

$$\begin{aligned} P_i(k) - \bar{\gamma} &< M z_i^{\gamma^{\geq}}(k), \\ -P_i(k) + \bar{\gamma} &\leq M(1 - z_i^{\gamma^{\geq}}(k)); \end{aligned} \tag{3a}$$

$$\begin{aligned} -P_i(k) + \bar{\gamma} &< M z_i^{\gamma^{\leq}}(k), \\ P_i(k) - \bar{\gamma} &\leq M(1 - z_i^{\gamma^{\leq}}(k)); \end{aligned} \tag{3b}$$

where M is a sufficiently large positive number. The auxiliary variables codified by inequalities (3) are then adopted to model the MLD linking the discrete logical states of each device with its operating power, according to (1). Namely, for $i \in \{e, f\}$, the following constraints are derived

$$(1 - \delta_i^{\alpha}(k)) + z_i^{\gamma^{\geq}}(k) \geq 1, \tag{4a}$$

$$(1 - \delta_i^{\alpha}(k)) + z_i^{\gamma^{\leq}}(k) \geq 1. \tag{4b}$$

The mathematical formulation of these constraints is reported, for the reader's convenience, in Appendix A.1. Since all the states are discrete and the devices will work only in one and only one mode at any time k, the additional constraint

$$\delta_i^{\mathrm{OFF}}(k) + \delta_i^{\mathrm{CLD}}(k) + \delta_i^{\mathrm{STB}}(k) + \delta_i^{\mathrm{WRM}}(k) + \delta_i^{\mathrm{ON}}(k) = 1 \tag{5}$$

has to be considered

4.1.2 Mathematical Model and MLD Constraints Formulation of the State Transitions

As discussed above, the devices models are characterized by five discrete operational states. These operational states imply twenty possible mode transitions for each device by following expressions

$$\sigma_{\alpha_i}^{\beta}(k) = \delta_i^{\alpha}(k-1) \wedge \delta_i^{\beta}(k), \tag{6}$$

with $\sigma_{\alpha_i}^{\beta} \in [0,1]$, $\alpha, \beta \in \{\mathrm{OFF}, \mathrm{CLD}, \mathrm{STB}, \mathrm{WRM}, \mathrm{ON}\}$ and $\alpha \neq \beta$. Based on the relationships defined by Bemporad and Morari [4] that take into account MIL constraints, each expression of (6) is equivalently converted into three inequalities and introduced as constraints in the proposed MPC controller, thus resulting in the following formulas:

$$\begin{aligned} -\delta_i^{\alpha}(k-1) + \sigma_{\alpha_i}^{\beta}(k) &\leq 0, \\ -\delta_i^{\beta}(k) + \sigma_{\alpha_i}^{\beta}(k) &\leq 0, \\ \delta_i^{\alpha}(k-1) + \delta_i^{\beta}(k) - \sigma_{\alpha_i}^{\beta}(k) &\leq 1. \end{aligned} \tag{7}$$

The extended version of (7) is reported in the Appendix (A.2) for reference. It is important to highlight that, for some state transitions, i.e., $\sigma_{\mathrm{ON}_i}^{\mathrm{OFF}}(k)$, $\sigma_{\mathrm{OFF}_i}^{\mathrm{CLD}}(k)$ and $\sigma_{\mathrm{STB}_i}^{\mathrm{OFF}}(k)$, a cost is paid due to the stack degradation in switching from hydrogen production/consumption, not production/consumption and vice versa. These transitions will be included in the devices cost functions while all the inadmissible transitions, i.e., those not shown in Figure 2, are set to zero resulting in the further constraints

$$\sigma_{\mathrm{OFF},i}^{\mathrm{STB}}(k) = \sigma_{\mathrm{OFF},i}^{\mathrm{WRM}}(k) = \sigma_{\mathrm{OFF},i}^{\mathrm{ON}}(k) = 0, \tag{8a}$$
$$\sigma_{\mathrm{CLD},i}^{\mathrm{OFF}}(k) = \sigma_{\mathrm{CLD},i}^{\mathrm{WRM}}(k) = \sigma_{\mathrm{CLD},i}^{\mathrm{ON}}(k) = 0, \tag{8b}$$
$$\sigma_{\mathrm{STB},i}^{\mathrm{ON}}(k) = \sigma_{\mathrm{STB},i}^{\mathrm{CLD}}(k) = 0, \tag{8c}$$
$$\sigma_{\mathrm{WRM},i}^{\mathrm{OFF}}(k) = \sigma_{\mathrm{WRM},i}^{\mathrm{CLD}}(k) = \sigma_{\mathrm{WRM},i}^{\mathrm{STB}}(k) = 0, \tag{8d}$$
$$\sigma_{\mathrm{ON},i}^{\mathrm{CLD}}(k) = \sigma_{\mathrm{ON},i}^{\mathrm{WRM}}(k) = 0, \tag{8e}$$

that will be included into the proposed controller.

4.2 Hydrogen dynamics model

Hydrogen dynamics are described by the state variable $H(k)$, where η_{e} and η_{f} are the efficiencies of the electrolyzer and of the fuel cell, respectively, and $H(k)$ is the hydrogen level in the tank. Then,

$$H(k+1) = H(k) + \eta_{\mathrm{e}} P_{\mathrm{e}}(k) \delta_{\mathrm{e}}^{\mathrm{ON}}(k) T_s - \frac{P_{\mathrm{f}}(k) \delta_{\mathrm{f}}^{\mathrm{ON}}(k) T_s}{\eta_{\mathrm{f}}}, \tag{9a}$$

where T_s is the sampling period. Notice that, according to (9) the electrolyzer and the fuel cell respectively produces and consumes hydrogen only in their ON modes.

4.3 Temporal constraints for cold and warm starts

The automata depicted in Figure 2 include the two states CLD and WRM for each $i \in \{\mathrm{e}, \mathrm{f}\}$ in order to include the electrolyzer and the fuel cell cold and warm starts as two different temporal constraints for each device. In fact, transitions from off to stand-by and transitions from stand-by to on happens within two different time ranges (typically cold starts take more time than warm starts).

Then, the needed temporal constraints can be defined through inequalities involving $\delta_i^{\alpha}(k)$, for each $i \in \{\mathrm{e}, \mathrm{f}\}$ and with $\alpha \in \{\mathrm{CLD}, \mathrm{WRM}\}$, as

$$\delta_i^{\mathrm{CLD}}(k) - \delta_i^{\mathrm{CLD}}(k-1) \leq \delta_i^{\mathrm{CLD}}(\tau^{\mathrm{CLD}}), \tag{10a}$$

$$\delta_i^{\mathrm{CLD}}(k) + \delta_i^{\mathrm{CLD}}(k-1) + \cdots + \delta_i^{\mathrm{CLD}}(k - T^{\mathrm{CLD}}) \leq T^{\mathrm{CLD}}, \tag{10b}$$

$$\delta_i^{\mathrm{WRM}}(k) - \delta_i^{\mathrm{WRM}}(k-1) \leq \delta_i^{\mathrm{WRM}}(\tau^{\mathrm{WRM}}), \tag{10c}$$

$$\delta_i^{\mathrm{WRM}}(k) + \delta_i^{\mathrm{WRM}}(k-1) + \cdots + \delta_i^{\mathrm{WRM}}(k - T^{\mathrm{WRM}}) \leq T^{\mathrm{WRM}}, \tag{10d}$$

with $i \in \{\mathrm{ez}, \mathrm{fc}\}$ and where T^{CLD}, T^{WRM} are the start up time (cold start) and response time (warm start) that each devices has to wait before a commutation from OFF to ON and from STB to ON, respectively, see Figure. 2 and τ^{CLD} and τ^{WRM} are two temporal parameters chosen as

$$\tau^{\mathrm{WRM}} = k+1, \ldots, \min(k + T^{\mathrm{WRM}} - 1, T), \tag{11a}$$

$$\tau^{\mathrm{CLD}} = k+1, \ldots, \min(k + T^{\mathrm{CLD}} - 1, T), \tag{11b}$$

where T is the simulation horizon.

4.4 Ramp up constraints

In order not to damage the electrolyzer and the fuel cell during their operations, the controller will force the P_{e} and P_{f} per time-step variation to be bounded according to

$$\left|P_{\mathrm{e}}(k) - P_{\mathrm{e}}(k-1)\right| \delta_{\mathrm{e}}^{\mathrm{ON}}(k) \leq R_{\mathrm{e}}, \tag{12a}$$

$$\left|P_{\mathrm{f}}(k) - P_{\mathrm{f}}(k-1)\right| \delta_{\mathrm{f}}^{\mathrm{ON}}(k) \leq R_{\mathrm{f}}, \tag{12b}$$

where R_{e} and R_{f} are the ramp limits of the electrolyzer and the fuel cell, respectively.

4.5 Power balance constraints

According to Figure 1 the power balance is

$$P_w(k) - P_{\mathrm{e}}(k)\delta_{\mathrm{e}}^{\mathrm{ON}}(k) + P_{\mathrm{f}}(k)\delta_{\mathrm{f}}^{\mathrm{ON}}(k) - P_{\mathrm{avl}}(k) = 0, \tag{13}$$

where $P_e(k)\delta_e^{\mathrm{ON}}(k) = P_e^{\mathrm{in}}$ and $P_f(k)\delta_f^{\mathrm{ON}}(k) = P_f^{\mathrm{out}}$. The power balance highlights that the available power P_{avl} depends on the power P_w achieved through wind generation and the balancing action of the hydrogen storage system and the dumping load.

4.6 Operating range constraints

The electrolyzer, the fuel cell and the hydrogen tank have operating ranges limits that can be modeled correspondingly as

$$P_{\mathrm{e}}^{\min} \leq P_{\mathrm{e}}(k) \leq P_{\mathrm{e}}^{\max}, \tag{14a}$$
$$P_{\mathrm{f}}^{\min} \leq P_{\mathrm{f}}(k) \leq P_{\mathrm{f}}^{\max}, \tag{14b}$$
$$H^{\min} \leq H(k) \leq H^{\max}, \tag{14c}$$

where $P_{\mathrm{e}}^{\min}$ is the minimum input power of the electrolyzer, $P_{\mathrm{e}}^{\max}$ is the maximum input power of the electrolyzer, $P_{\mathrm{f}}^{\min}$ is the minimum output power of the fuel cell, $P_{\mathrm{f}}^{\max}$ is the maximum output power of the fuel cell, $H^{\min}$ is the minimum hydrogen level to be retained within the tank and $H^{\max}$ is the maximum hydrogen level that the tank can withtstand.

5 Problem Description

In this section the proposed MPC problem for output power smoothing and grid operator reference tracking is presented by exploiting the sequentially execution of control technique. We define the cost functions of the electrolyzer and to the fuel cell, operations, then the cost function for tracking the reference of the grid operator and we define the cost function for the output power smoothing. The multi-objective optimization is set-up in a sequential fashion, by giving priority first to the output power smoothing and then to the tracking at the minimum cost. Furthermore, the overall system is also subject to hard constraints in terms of energy storage system requirements, ramp rate requirements and sequential operational modes of the storage system.

5.1 Electrolyzer and Fuel cell Cost Functions

The cost functions that model the electrolyzer and the fuel cell operating costs include several terms accounting for the component depreciation, the reduction of life cycles (weighting the three switching characterizing a cycle), the energy spent in keeping the units warm during stand-by, the energy spent for cold starts and the energy spent for warm starts. The fluctuating loads and the operating cycles can seriously affect these devices in a number of ways. Therefore, in order to tackle such problems, we propose the following cost functions

$$\begin{aligned} \mathrm{J}_i(k) := & \left(\frac{S_{\mathrm{rep},i}}{\mathrm{NH}_i} + \mathrm{Cost}_i^{\mathrm{OM}} \right) \delta_i^{\mathrm{ON}}(k) \\ & + \mathrm{Cost}_{\mathrm{ON}_i}^{\mathrm{OFF}} \sigma_{\mathrm{ON}_{\mathrm{ez}}}^{\mathrm{OFF}}(k) + \mathrm{Cost}_{\mathrm{CLD}_i}^{\mathrm{STB}} \sigma_{\mathrm{CLD}_i}^{\mathrm{STB}}(k) + \mathrm{Cost}_{\mathrm{STB}_i}^{\mathrm{OFF}} \sigma_{\mathrm{STB}_i}^{\mathrm{OFF}}(k) \\ & + c(k) P_i^{\mathrm{STB}} \delta_i^{\mathrm{STB}}(k) + c(k) P_i^{\mathrm{CLD}} \delta_i^{\mathrm{CLD}}(k) + c(k) P_i^{\mathrm{WRM}} \delta_i^{\mathrm{WRM}}(k), \end{aligned} \tag{15a}$$

where $\mathrm{Cost}_i^{\mathrm{OM}}$ indicates the devices operating and maintenance cost, and $c(k)$ is the power spot price that is the one hour price of wholesale market electricity. $\mathrm{Cost}_{\mathrm{ON}_i}^{\mathrm{OFF}}$, $\mathrm{Cost}_{\mathrm{CLD}_i}^{\mathrm{STB}}$, and $\mathrm{Cost}_{\mathrm{STB}_i}^{\mathrm{OFF}}$, denotes the cycle costs, respectively choosing $i \in \{\mathrm{ez}, \mathrm{fc}\}$. These costs are payed

any time a mode transition occurs, since any complete sequence of switching accounts for a working cycle and, therefore, reduces the components' life. We wish to emphasize, for the sake of clarity, that the cold start presents usually a higher cost than the one from STB to ON (warm start). On the other hand, devices in OFF mode do not absorb any power, while this is not true in STB, CLD, and WRM modes. The $S_{\mathrm{rep,ez}}$ and $S_{\mathrm{rep,fc}}$ represents the stack replacement cost of the electrolyzer and the fuel cell, respectively.

5.2 Grid Operator Reference Tracking Cost Function

One goal of the system is to track the reference P_{ref} from the grid operator with the available power P_{avl} in the best possible and economical way. The tracking cost function is given by the mismatch between P_{ref} and P_{avl} as

$$J_l(k) := \sum_{k=0}^{T-1} \Big(P_{\mathrm{avl}}(k) - P_{\mathrm{ref}}(k) \Big)^2. \tag{16}$$

5.3 Output Power Smoothing Cost Function

The output power smoothing cost function is presented in this section. In order to participate in the electricity markets, the smooth supply of the power plan scheduled with the grid operator(s) is mandatory. In our study, the output power smoothing has been achieved by accounting previous available power values, and accordingly evaluating the scheduling of future power ahead in time. The output power smoothing is formulated so that the controller will minimize the cost function

$$J_s := \sum_{k=0}^{T-1} \sum_{\tau=1}^{\tau_B} \omega^{k,\tau} y^{k,\tau}, \tag{17}$$

where τ_B is the number of the previous samples considered for the smoothing action, $\omega^{k,\tau}$ defines a weighting factor with $\sum_{\tau=1}^{\tau_B} \omega^{k,\tau} = 1$, and $y^{k,\tau}$ is a decision variable that defines the bound on the difference of past and future available power values $|P_{\mathrm{avl}}(k) - P_{\mathrm{avl}}(k-\tau)|$. The decision variable $y^{k,\tau}$ is subjected to the following constraints

$$y^{k,\tau} \geq 0, \tag{18a}$$

$$y^{k,\tau} \geq |P_{\mathrm{avl}}(k) - P_{\mathrm{avl}}(k-\tau)| - \bar{y}^{\tau}, \tag{18b}$$

where $\bar{y}^{\tau}$ is a threshold below which the power span is considered acceptable by the grid operator, *i. e.* the power provided is considered "smooth".

5.4 Multi-objective Proposed MPC controller formulation

Because of the complexity of the system in terms of number of inputs, outputs and decision variables, an MPC scheme, as that reported in Figure 3, seems a natural choice. Indeed, the main idea of the MPC is to exploit the models of dynamic systems under control in order to predict their future evolution within a prediction horizon. Based on this prediction, at each step k the controller selects a sequence of future command inputs through an optimization

procedure, which aims at minimizing suitable cost functions and enforcing the fulfillment of the required constraints. Only the first element of such sequence, i.e. the control input at time k, is applied while at the next sampling time the new state of the system is measured and a new constrained optimization problem is solved again. Interestingly, the constrained optimization step naturally allows to include also logical dynamical systems within the formulation, making the MPC scheme relevant for a quite wide class of control problems.

5.4.1 MPC formulation for the energy-storage use case

In order to present the MPC policy, let us just consider the hydrogen dynamics in (9) and let us denote by $H(k+j \mid k)$, with $j > 0$, the corresponding state variables at time $k+j$ predicted at time k by means of (9) as well. At each k, given the initial state $H(k)$, the MPC provides the optimal control sequences

$$\mathscr{C}_k := \left\{ y_k^{T-1}, P_{\mathrm{i},k}^{T-1}, P_{\mathrm{avl},k}^{T-1}, \delta_{\mathrm{i},k}^{\alpha,T-1}, \sigma_{\alpha,\mathrm{i},k}^{\beta,T-1}, z_{\mathrm{i},k}^{\gamma,T-1} \right\}, \tag{19}$$

with the proposed optimal multi-objective controller defined as

$$\begin{aligned}
&\min_{\mathscr{C}_k} \left\{ J_s,\ J \right\} \\
&\text{s.t.} \\
&\quad \text{Discrete logical states,} \\
&\quad \text{Mode transitions,} \\
&\quad \text{Operating constraints,} \\
&\quad \text{Ramp Up constraints,} \\
&\quad \text{Storage dynamics,} \\
&\quad \text{Physical constraints,} \\
&\quad \text{Smoothing constraints,} \\
&\quad \delta_i^{\alpha} \in [0,1], \qquad \alpha \in \{\mathrm{ON}, \mathrm{CLD}, \mathrm{STB}, \mathrm{WRM}, \mathrm{OFF}\}, \\
&\quad \delta_{\alpha_i}^{\beta} \in [0,1], \qquad \alpha, \beta \in \{\mathrm{ON}, \mathrm{CLD}, \mathrm{STB}, \mathrm{WRM}, \mathrm{OFF}\}, \\
&\quad z_i^{\gamma} \in \{0,1\}, \qquad \gamma \in \{\geq 0, \leq 0, \ldots, \leq P_i^{\max}\}, i \in \{\mathrm{ez}, \mathrm{fc}\},
\end{aligned} \tag{20}$$

where T is the the simulation horizon. The mathematical formulations of (18) and (19) are reported, for the reader convenience, in the Appendix A.3.

5.5 Implementation and Solving the Optimization Problem

The diagram of the controller is detailed in Figure 3. The MPC controller formulation was implemented in MATLAB/YALMIP using the solver ILOG's CPLEX 12.8; all computations are performed on a laptop with an Intel Core (TM) *i*7 – 7700HQ 2.8 GHz processor and 16 GB of memory. The MPC is tuned giving bigger weights to degradation cost of the fuel cell and the electrolyzer, since these devices are sensitive to degradation. To finalize the controller setup, the T is taken as 24 h with 1 h sampling period T_s.

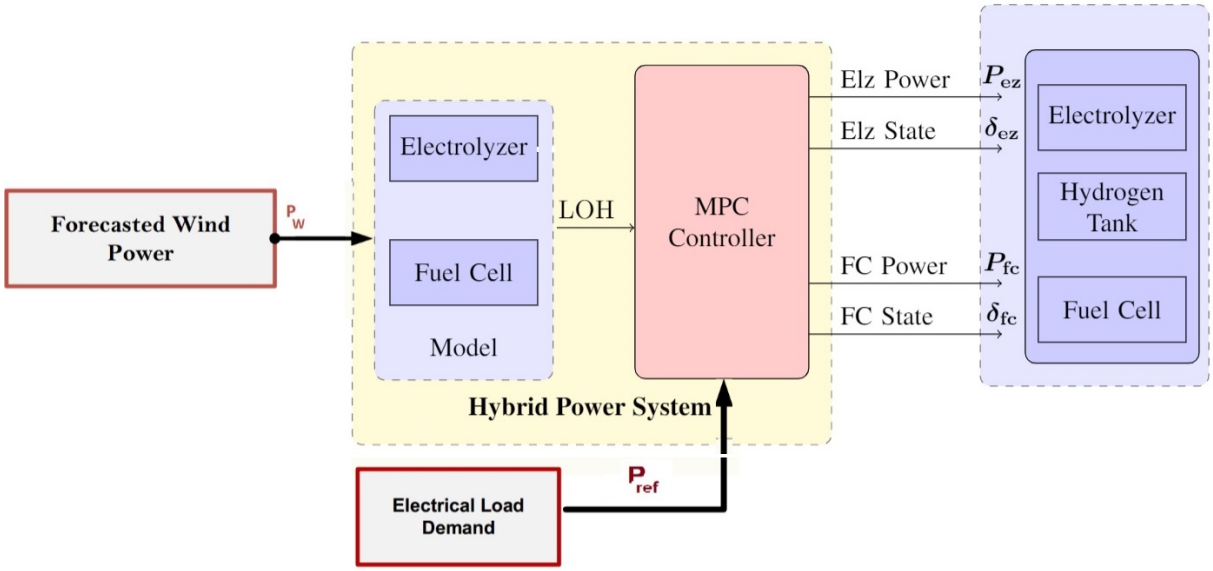

Figure 3: Proposed MPC Control Scheme.

6 Simulations and Numerical Results

The aim of this study is to design a controller, based on model predictive control (MPC) technique, to smooth the output power, which has been computed with the help of (13), and subject to a variety of constraints on the system model. The proposed controller is capable of smoothing the output by taking the past power values and taking the decision variables ahead in time. The overall effect aims at smoothing the output power with respect to the past values under practical constraints. We illustrate the effectiveness of the proposed MPC controller with a simulation example, employing real wind farm data under a variety of hard constraints.

Numerous experiments have been performed to find out the optimal parameters, as a case study results from one of the experiments are presented where optimized results are presented for 4-steps ahead predictions based on the accuracy of the prediction model for our particular case.

6.1 Reference Tracking with Output Power smoothing

In order to test the system, the optimally computed smoothed signal is then applied to a power grid operator reference tracking problem. The tuning of the grid operator tracking cost function weights seeks for a soft tracking of the output variables towards the given references and an efficient use of the stored energy. More specifically, if there exists a big difference between the grid operator energy and the energy available in the system, the controller operates the ESS in order to track the grid operator reference however with a major preference for minimizing operating costs. Accordingly, the prioritization weights ρ_l, ρ_e and ρ_f have been adjusted by trial and error. In the simulations, $H(0) = 4$ kg is considered as the initial level of the hydrogen in the tank. The results are summarized in the Figure. 4. In this numerical example, the results from the sequentially executed smoothing and the grid operator reference satisfy-

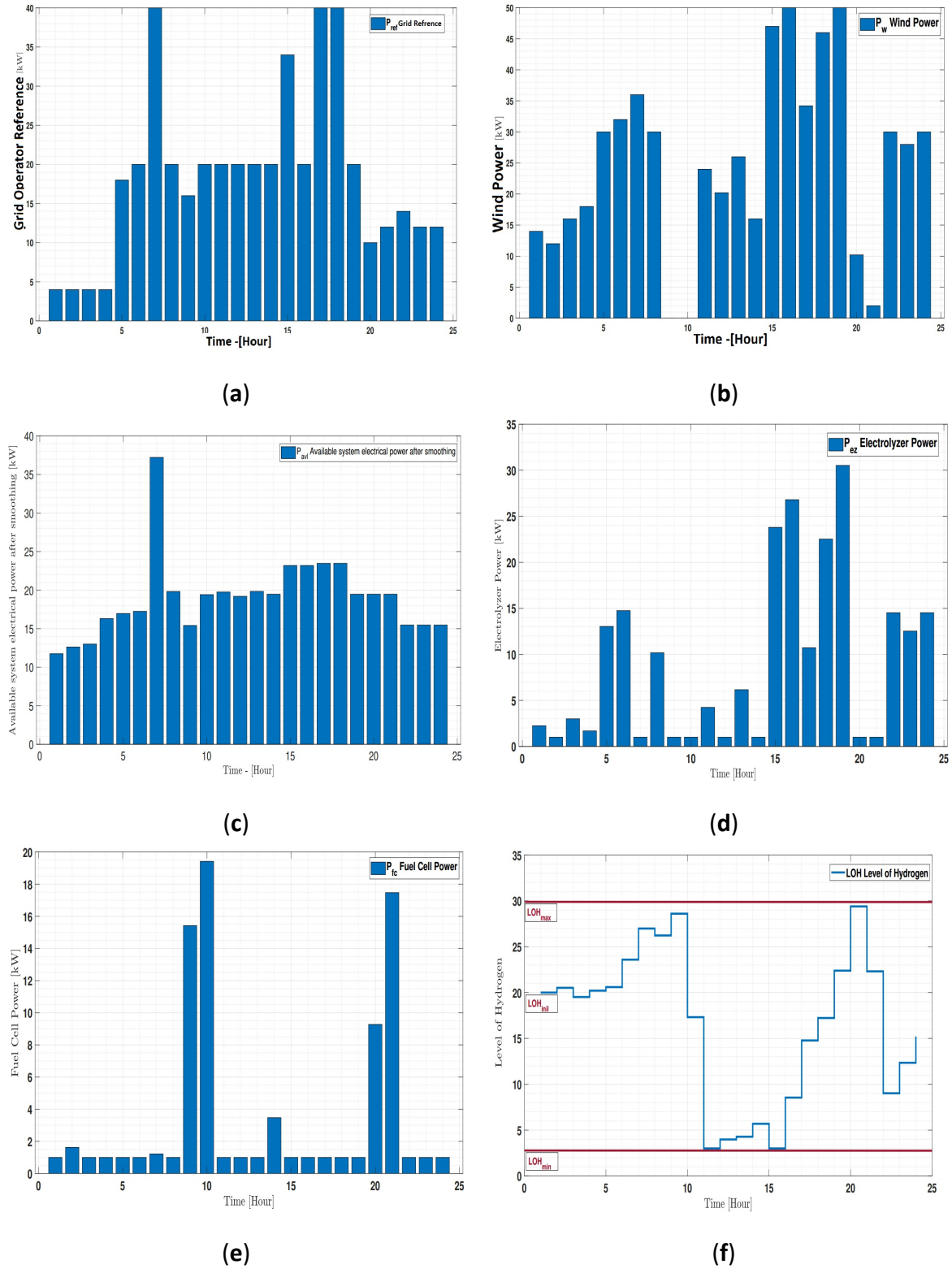

Figure 4: Numerical results for Example 1. (a) Grid Operator Reference. (b) Forecasted Wind Power. (c) Available Power delivered to the grid after smoothing. (d) Power of the Electrolyzer. (e) Power of the Fuel Cell. (f) Level of Hydrogen.

ing optimization has been presented. The grid operator reference has been tracked with the help of optimally computed smoothed signal and both exceeding and missing power are considered, with a power flow towards or from the storage. In order to show the effectiveness of the implemented algorithm, the devices switching states have been shown for a case with frequent imbalances between the grid operator reference and the wind power over the 24 hours simulation. Figure 4 (a), (b) shows the grid operator reference P_{ref} and the wind power P_w, respectively. It can be seen that the difference between the wind power and the reference of grid operator is mismatched frequently over the 24 hours simulation. The controller tries to track the grid operator reference as much as possible with the availability of the wind power and the smooth power available in the system for each time step k.

As per working principle of the electrolyzer, the exceeding power$(P_w - P_{\mathrm{ref}})$ is shunted to the electrolyzer (which was set by the controller to its ON state) for the production of hydrogen according to the current LOH and the storage physical constraints Figure. 4(d). Figure. 4(f) explains that the level of hydrogen in the storage has increased according to the storage constraints from $H^{\min}$ to $H^{\max}$ during the excess wind hours. Figure. 4(e) shows the fuel cell power. It can be clearly seen from 4(e) that the fuel cell does not supply power (in its OFF state) to the grid when the wind power availability is higher than the grid operator reference. It is important to note that the controller is designed to switch the electrolyzer and the fuel cell to their STB state if it predicts the need to switch them on again in the near future, i.e., hours and for the electrolyzer and hour 8 for the fuel cell.

7 Conclusions

The current deliverable develops the high-level control algorithm of the integrated wind-hydrogen based ESS in HAEOLUS for the energy-storage use case [1], [2].

The proposed controller architecture relies upon an MPC control scheme and uses models with discrete logical states representing operating device modes and continuous dynamics. The models take into account the costs that each device introduces any time it switches between operating mode, which cause life cycles reduction and efficiency degradation. Furthermore, other physical constraints and costs, such as the power consumptions in stand-by, are also taken into account.

The MPC controller architecture feature a two step optimization where the first goal is the achievement of the optimal available power increment such that the weighted average of all increments within certain time windows is minimum. Such an optimal value is then plugged into the second step optimization stage as a constraint to be fulfilled while minimizing the grid operator reference tracking cost function.

All the models reported in this deliverable have been implemented in MATLAB. The optimizations have been performed through YALMIP.

A Appendix A

A.1 Mathematical Model and Constraints Formulation of the Logical States

In order to include (1) within an optimal control framework, the cases need further manipulations to derive MILP constraints. For this reason, as intermediate step, we introduce the following 20 auxiliary Boolean variables $z_i^{\gamma}(k) \in \{0,1\}$, with $i \in \{\mathrm{e},\mathrm{f}\}$ and $\gamma \in \{\geq 0, \leq 0, \geq P_i^{\mathrm{CLD}}, \leq P_i^{\mathrm{CLD}}, \geq P_i^{\mathrm{STB}}, \leq P_i^{\mathrm{STB}}, \geq P_i^{\mathrm{WRM}}, \leq P_i^{\mathrm{WRM}}, \geq P_i^{\mathrm{min}}, \leq P_i^{\mathrm{max}}\}$, for each k [4]:

$$z_i^{\geq 0}(k) = \begin{cases} 1 & P_i(k) \geq 0, \\ 0 & P_i(k) < 0, \end{cases} \tag{21a}$$

$$z_i^{\leq 0}(k) = \begin{cases} 0 & P_i(k) > 0, \\ 1 & P_i(k) \leq 0, \end{cases} \tag{21b}$$

$$z_i^{\geq P_i^{\mathrm{CLD}}}(k) = \begin{cases} 1 & P_i(k) \geq P_i^{\mathrm{CLD}}, \\ 0 & P_i(k) < P_i^{\mathrm{CLD}}, \end{cases} \tag{21c}$$

$$z_i^{\leq P_i^{\mathrm{CLD}}}(k) = \begin{cases} 0 & P_i(k) > P_i^{\mathrm{CLD}}, \\ 1 & P_i(k) \leq P_i^{\mathrm{CLD}}, \end{cases} \tag{21d}$$

$$z_i^{\geq P_i^{\mathrm{STB}}}(k) = \begin{cases} 1 & P_i(k) \geq P_i^{\mathrm{STB}}, \\ 0 & P_i(k) < P_i^{\mathrm{STB}}, \end{cases} \tag{21e}$$

$$z_i^{\leq P_i^{\mathrm{STB}}}(k) = \begin{cases} 0 & P_i(k) > P_i^{\mathrm{STB}}, \\ 1 & P_i(k) \leq P_i^{\mathrm{STB}}, \end{cases} \tag{21f}$$

$$z_i^{\geq P_i^{\mathrm{WRM}}}(k) = \begin{cases} 1 & P_i(k) \geq P_i^{\mathrm{WRM}}, \\ 0 & P_i(k) < P_i^{\mathrm{WRM}}, \end{cases} \tag{21g}$$

$$z_i^{\leq P_i^{\mathrm{WRM}}}(k) = \begin{cases} 0 & P_i(k) > P_i^{\mathrm{WRM}}, \\ 1 & P_i(k) \leq P_i^{\mathrm{WRM}}, \end{cases} \tag{21h}$$

$$z_i^{\geq P_i^{\mathrm{min}}}(k) = \begin{cases} 1 & P_i(k) \geq P_i^{\mathrm{min}}, \\ 0 & P_i(k) < P_i^{\mathrm{min}}, \end{cases} \tag{21i}$$

$$z_i^{\leq P_i^{\mathrm{max}}}(k) = \begin{cases} 0 & P_i(k) > P_i^{\mathrm{max}}, \\ 1 & P_i(k) \leq P_i^{\mathrm{max}}. \end{cases} \tag{21j}$$

By using the transformations defined in (21), the above formulas can be expressed with the following boolean inequalities

$$\begin{aligned} P_i(k) &< M z_i^{\geq 0}(k), \\ -P_i(k) &\leq M(1 - z_i^{\geq 0}(k)); \end{aligned} \tag{22a}$$

$$\begin{aligned} -P_i(k) &< M z_i^{\leq 0}(k), \\ P_i(k) &\leq M(1 - z_i^{\leq 0}(k)); \end{aligned} \tag{22b}$$

$$P_i(k) - P_i^{\mathrm{CLD}} < M z_i^{\geq P_i^{\mathrm{CLD}}}(k), \quad -P_i(k) + P_i^{\mathrm{CLD}} \leq M(1 - z_i^{\geq P_i^{\mathrm{CLD}}}(k)); \tag{22c}$$

$$-P_i(k) + P_i^{\mathrm{CLD}} < M z_i^{\leq P_i^{\mathrm{CLD}}}(k), \quad P_i(k) - P_i^{\mathrm{CLD}} \leq M(1 - z_i^{\leq P_i^{\mathrm{CLD}}}(k)); \tag{22d}$$

$$P_i(k) - P_i^{\mathrm{STB}} < M z_i^{\geq P_i^{\mathrm{STB}}}(k), \quad -P_i(k) + P_i^{\mathrm{STB}} \leq M(1 - z_i^{\geq P_i^{\mathrm{STB}}}(k)); \tag{22e}$$

$$-P_i(k) + P_i^{\mathrm{STB}} < M z_i^{\leq P_i^{\mathrm{STB}}}(k), \quad P_i(k) - P_i^{\mathrm{STB}} \leq M(1 - z_i^{\leq P_i^{\mathrm{STB}}}(k)); \tag{22f}$$

$$P_i(k) - P_i^{\mathrm{WRM}} < M z_i^{\geq P_i^{\mathrm{STB}}}(k), \quad -P_i(k) + P_i^{\mathrm{WRM}} \leq M(1 - z_i^{\geq P_i^{\mathrm{STB}}}(k)); \tag{22g}$$

$$-P_i(k) + P_i^{\mathrm{WRM}} < M z_i^{\leq P_i^{\mathrm{WRM}}}(k), \quad P_i(k) - P_i^{\mathrm{WRM}} \leq M(1 - z_i^{\leq P_i^{\mathrm{WRM}}}(k)); \tag{22h}$$

$$P_i(k) - P_i^{\min} < M z_i^{\geq P_i^{\min}}(k), \quad -P_i(k) + P_i^{\min} \leq M(1 - z_i^{\geq P_i^{\min}}(k)); \tag{22i}$$

$$-P_i(k) + P_i^{\max} < M z_i^{\leq P_i^{\max}}(k), \quad P_i(k) - P_i^{\max} \leq M(1 - z_i^{\leq P_i^{\max}}(k)), \tag{22j}$$

where M is a suitably large positive number. The auxiliary variables in (22) are then exploited to model the mixed-logical dynamics by linking the discrete logical variables of each device with the corresponding operating power, according to (1). That is, the logical variables $\delta_i^{\alpha}(k)$ can be now determined in terms of $z_i^{\gamma}(k)$, for each $i \in \{\mathrm{e}, \mathrm{f}\}$, with $\alpha \in \{\mathrm{OFF}, \mathrm{CLD}, \mathrm{STB}, \mathrm{WRM}, \mathrm{ON}\}$ and $\gamma \in \{\geq 0, \leq 0, \geq P_i^{\mathrm{CLD}}, \leq P_i^{\mathrm{CLD}}, \geq P_i^{\mathrm{STB}}, \leq P_i^{\mathrm{STB}}, \geq P_i^{\mathrm{WRM}}, \leq P_i^{\mathrm{WRM}}, \geq P_i^{\min}, \leq P_i^{\max}\}$, by means of

$$\left(1 - \delta_i^{\mathrm{ON}}(k)\right) + z_i^{\geq P_i^{\min}}(k) \geq 1, \tag{23a}$$

$$\left(1 - \delta_i^{\mathrm{ON}}(k)\right) + z_i^{\leq P_i^{\max}}(k) \geq 1, \tag{23b}$$

$$\left(1 - \delta_i^{\mathrm{CLD}}(k)\right) + z_i^{\geq P_i^{\mathrm{CLD}}}(k) \geq 1, \tag{23c}$$

$$\left(1 - \delta_i^{\mathrm{CLD}}(k)\right) + z_i^{\leq P_i^{\mathrm{CLD}}}(k) \geq 1, \tag{23d}$$

$$\left(1 - \delta_i^{\mathrm{STB}}(k)\right) + z_i^{\geq P_i^{\mathrm{STB}}}(k) \geq 1, \tag{23e}$$

$$\left(1-\delta_i^{\mathrm{STB}}(k)\right)+z_i^{\leq P_i^{\mathrm{STB}}}(k)\geq 1, \tag{23f}$$

$$\left(1-\delta_i^{\mathrm{WRM}}(k)\right)+z_i^{\geq P_i^{\mathrm{WRM}}}(k)\geq 1, \tag{23g}$$

$$\left(1-\delta_i^{\mathrm{WRM}}(k)\right)+z_i^{\leq P_i^{\mathrm{WRM}}}(k)\geq 1, \tag{23h}$$

$$\left(1-\delta_i^{\mathrm{OFF}}(k)\right)+z_i^{\geq 0}(k)\geq 1, \tag{23i}$$

$$\left(1-\delta_i^{\mathrm{OFF}}(k)\right)+z_i^{\leq 0}(k)\geq 1, \tag{23j}$$

Since all the states are discrete and the devices will work only in one and only one mode at a time k, which results in consideration of the following (mutually exclusive) constraint

$$\delta_i^{\mathrm{ON}}(k)+\delta_i^{\mathrm{OFF}}(k)+\delta_i^{\mathrm{STB}}(k)+\delta_i^{\mathrm{CLD}}(k)+\delta_i^{\mathrm{WRM}}(k)=1. \tag{24}$$

A.2 Mathematical Model and Constraints Formulation of the State Transitions

As discussed above, the devices models are characterized by five discrete operational states. These operational states imply twenty possible mode transitions for each device. In what follows, we define all of the transitions contributing to the cost functions described in (24), and all the transitions that are not allowed for the devices, and thus not appearing in the sequential graph

$$\sigma_{\mathrm{OFF},i}^{\mathrm{ON}}(k)=\delta_i^{\mathrm{OFF}}(k-1)\wedge\delta_i^{\mathrm{ON}}(k), \tag{25a}$$

$$\sigma_{\mathrm{OFF},i}^{\mathrm{WRM}}(k)=\delta_i^{\mathrm{OFF}}(k-1)\wedge\delta_i^{\mathrm{WRM}}(k), \tag{25b}$$

$$\sigma_{\mathrm{OFF},i}^{\mathrm{STB}}(k)=\delta_i^{\mathrm{OFF}}(k-1)\wedge\delta_i^{\mathrm{STB}}(k), \tag{25c}$$

$$\sigma_{\mathrm{CLD},i}^{\mathrm{OFF}}(k)=\delta_i^{\mathrm{CLD}}(k-1)\wedge\delta_i^{\mathrm{OFF}}(k), \tag{25d}$$

$$\sigma_{\mathrm{CLD},i}^{\mathrm{ON}}(k)=\delta_i^{\mathrm{CLD}}(k-1)\wedge\delta_i^{\mathrm{ON}}(k), \tag{25e}$$

$$\sigma_{\mathrm{CLD},i}^{\mathrm{WRM}}(k)=\delta_i^{\mathrm{CLD}}(k-1)\wedge\delta_i^{\mathrm{WRM}}(k), \tag{25f}$$

$$\sigma_{\mathrm{STB},i}^{\mathrm{ON}}(k)=\delta_i^{\mathrm{STB}}(k-1)\wedge\delta_i^{\mathrm{ON}}(k), \tag{25g}$$

$$\sigma_{\mathrm{STB},i}^{\mathrm{CLD}}(k)=\delta_i^{\mathrm{STB}}(k-1)\wedge\delta_i^{\mathrm{CLD}}(k), \tag{25h}$$

$$\sigma_{\mathrm{WRM},i}^{\mathrm{OFF}}(k)=\delta_i^{\mathrm{WRM}}(k-1)\wedge\delta_i^{\mathrm{OFF}}(k), \tag{25i}$$

$$\sigma_{\mathrm{WRM},i}^{\mathrm{CLD}}(k)=\delta_i^{\mathrm{WRM}}(k-1)\wedge\delta_i^{\mathrm{CLD}}(k), \tag{25j}$$

$$\sigma_{\mathrm{WRM},i}^{\mathrm{STB}}(k)=\delta_i^{\mathrm{WRM}}(k-1)\wedge\delta_i^{\mathrm{STB}}(k), \tag{25k}$$

$$\sigma_{\mathrm{ON},i}^{\mathrm{CLD}}(k)=\delta_i^{\mathrm{ON}}(k-1)\wedge\delta_i^{\mathrm{CLD}}(k), \tag{25l}$$

$$\sigma_{\mathrm{ON},i}^{\mathrm{WRM}}(k)=\delta_i^{\mathrm{ON}}(k-1)\wedge\delta_i^{\mathrm{WRM}}(k), \tag{25m}$$

$$\sigma_{\mathrm{CLD},i}^{\mathrm{STB}}(k)=\delta_i^{\mathrm{CLD}}(k-1)\wedge\delta_i^{\mathrm{STB}}(k), \tag{25n}$$

$$\sigma^{\mathrm{OFF}}_{\mathrm{STB},i}(k) = \delta^{\mathrm{STB}}_i(k-1) \wedge \delta^{\mathrm{OFF}}_i(k), \tag{25o}$$

$$\sigma^{\mathrm{OFF}}_{\mathrm{ON},i}(k) = \delta^{\mathrm{ON}}_i(k-1) \wedge \delta^{\mathrm{OFF}}_i(k), \tag{25p}$$

where $i \in \{\mathrm{e}, \mathrm{f}\}$, $\alpha, \beta \in \{\mathrm{OFF}, \mathrm{CLD}, \mathrm{STB}, \mathrm{WRM}, \mathrm{ON}\}$ and $\alpha \neq \beta$. Based on the relationships defined by Bemporad and Morari [4] that take into account mixed-integer linear constraints, each expression of the (25) is equivalently converted into three inequalities and introduced in the constraints of MPC controller, thus resulting in the 48 following inequalities:

$$\begin{aligned}
-\delta^{\mathrm{OFF}}_i(k-1) + \sigma^{\mathrm{ON}}_{\mathrm{OFF},i}(k) &\leq 0,\\
-\delta^{\mathrm{ON}}_i(k) + \sigma^{\mathrm{ON}}_{\mathrm{OFF},i}(k) &\leq 0,\\
\delta^{\mathrm{OFF}}_i(k-1) + \delta^{\mathrm{ON}}_i(k) - \sigma^{\mathrm{ON}}_{\mathrm{OFF},i}(k) &\leq 1;
\end{aligned} \tag{26a}$$

$$\begin{aligned}
-\delta^{\mathrm{OFF}}_i(k-1) + \sigma^{\mathrm{WRM}}_{\mathrm{OFF},i}(k) &\leq 0,\\
-\delta^{\mathrm{WRM}}_i(k) + \sigma^{\mathrm{WRM}}_{\mathrm{OFF},i}(k) &\leq 0,\\
\delta^{\mathrm{OFF}}_i(k-1) + \delta^{\mathrm{WRM}}_i(k) - \sigma^{\mathrm{WRM}}_{\mathrm{OFF},i}(k) &\leq 1;
\end{aligned} \tag{26b}$$

$$\begin{aligned}
-\delta^{\mathrm{OFF}}_i(k-1) + \sigma^{\mathrm{STB}}_{\mathrm{OFF},i}(k) &\leq 0,\\
-\delta^{\mathrm{STB}}_i(k) + \sigma^{\mathrm{STB}}_{\mathrm{OFF},i}(k) &\leq 0,\\
\delta^{\mathrm{OFF}}_i(k-1) + \delta^{\mathrm{STB}}_i(k) - \sigma^{\mathrm{STB}}_{\mathrm{OFF},i}(k) &\leq 1;
\end{aligned} \tag{26c}$$

$$\begin{aligned}
-\delta^{\mathrm{CLD}}_i(k-1) + \sigma^{\mathrm{OFF}}_{\mathrm{CLD},i}(k) &\leq 0,\\
-\delta^{\mathrm{OFF}}_i(k) + \sigma^{\mathrm{OFF}}_{\mathrm{CLD},i}(k) &\leq 0,\\
\delta^{\mathrm{CLD}}_i(k-1) + \delta^{\mathrm{OFF}}_i(k) - \sigma^{\mathrm{OFF}}_{\mathrm{CLD},i}(k) &\leq 1;
\end{aligned} \tag{26d}$$

$$\begin{aligned}
-\delta^{\mathrm{CLD}}_i(k-1) + \sigma^{\mathrm{ON}}_{\mathrm{CLD},i}(k) &\leq 0,\\
-\delta^{\mathrm{ON}}_i(k) + \sigma^{\mathrm{ON}}_{\mathrm{CLD},i}(k) &\leq 0,\\
\delta^{\mathrm{CLD}}_i(k-1) + \delta^{\mathrm{WRM}}_i(k) - \sigma^{\mathrm{ON}}_{\mathrm{CLD},i}(k) &\leq 1;
\end{aligned} \tag{26e}$$

$$\begin{aligned}
-\delta^{\mathrm{CLD}}_i(k-1) + \sigma^{\mathrm{WRM}}_{\mathrm{CLD},i}(k) &\leq 0,\\
-\delta^{\mathrm{WRM}}_i(k) + \sigma^{\mathrm{WRM}}_{\mathrm{CLD},i}(k) &\leq 0,\\
\delta^{\mathrm{CLD}}_i(k-1) + \delta^{\mathrm{WRM}}_i(k) - \sigma^{\mathrm{WRM}}_{\mathrm{CLD},i}(k) &\leq 1;
\end{aligned} \tag{26f}$$

$$\begin{aligned}
-\delta^{\mathrm{STB}}_i(k-1) + \sigma^{\mathrm{ON}}_{\mathrm{STB},i}(k) &\leq 0,\\
-\delta^{\mathrm{ON}}_i(k) + \sigma^{\mathrm{ON}}_{\mathrm{STB},i}(k) &\leq 0,\\
\delta^{\mathrm{STB}}_i(k-1) + \delta^{\mathrm{WRM}}_i(k) - \sigma^{\mathrm{ON}}_{\mathrm{STB},i}(k) &\leq 1;
\end{aligned} \tag{26g}$$

$$\begin{aligned}
-\delta^{\mathrm{STB}}_i(k-1) + \sigma^{\mathrm{CLD}}_{\mathrm{STB},i}(k) &\leq 0,\\
-\delta^{\mathrm{CLD}}_i(k) + \sigma^{\mathrm{CLD}}_{\mathrm{STB},i}(k) &\leq 0,\\
\delta^{\mathrm{STB}}_i(k-1) + \delta^{\mathrm{CLD}}_i(k) - \sigma^{\mathrm{CLD}}_{\mathrm{STB},i}(k) &\leq 1;
\end{aligned} \tag{26h}$$

$$
\begin{aligned}
-\delta_i^{\mathrm{WRM}}(k-1)+\sigma_{\mathrm{WRM},i}^{\mathrm{OFF}}(k)\leq 0,\\
-\delta_i^{\mathrm{OFF}}(k)+\sigma_{\mathrm{WRM},i}^{\mathrm{OFF}}(k)\leq 0,\\
\delta_i^{\mathrm{WRM}}(k-1)+\delta_i^{\mathrm{OFF}}(k)-\sigma_{\mathrm{WRM},i}^{\mathrm{OFF}}(k)\leq 1;
\end{aligned}
\tag{26i}
$$

$$
\begin{aligned}
-\delta_i^{\mathrm{WRM}}(k-1)+\sigma_{\mathrm{WRM},i}^{\mathrm{CLD}}(k)\leq 0,\\
-\delta_i^{\mathrm{CLD}}(k)+\sigma_{\mathrm{WRM},i}^{\mathrm{CLD}}(k)\leq 0,\\
\delta_i^{\mathrm{WRM}}(k-1)+\delta_i^{\mathrm{CLD}}(k)-\sigma_{\mathrm{WRM},i}^{\mathrm{CLD}}(k)\leq 1;
\end{aligned}
\tag{26j}
$$

$$
\begin{aligned}
-\delta_i^{\mathrm{WRM}}(k-1)+\sigma_{\mathrm{WRM},i}^{\mathrm{STB}}(k)\leq 0,\\
-\delta_i^{\mathrm{STB}}(k)+\sigma_{\mathrm{WRM},i}^{\mathrm{STB}}(k)\leq 0,\\
\delta_i^{\mathrm{WRM}}(k-1)+\delta_i^{\mathrm{STB}}(k)-\sigma_{\mathrm{WRM},i}^{\mathrm{STB}}(k)\leq 1;
\end{aligned}
\tag{26k}
$$

$$
\begin{aligned}
-\delta_i^{\mathrm{ON}}(k-1)+\sigma_{\mathrm{ON},i}^{\mathrm{CLD}}(k)\leq 0,\\
-\delta_i^{\mathrm{CLD}}(k)+\sigma_{\mathrm{ON},i}^{\mathrm{CLD}}(k)\leq 0,\\
\delta_i^{\mathrm{ON}}(k-1)+\delta_i^{\mathrm{CLD}}(k)-\sigma_{\mathrm{ON},i}^{\mathrm{CLD}}(k)\leq 1;
\end{aligned}
\tag{26l}
$$

$$
\begin{aligned}
-\delta_i^{\mathrm{ON}}(k-1)+\sigma_{\mathrm{ON},i}^{\mathrm{WRM}}(k)\leq 0,\\
-\delta_i^{\mathrm{WRM}}(k)+\sigma_{\mathrm{ON},i}^{\mathrm{WRM}}(k)\leq 0,\\
\delta_i^{\mathrm{ON}}(k-1)+\delta_i^{\mathrm{WRM}}(k)-\sigma_{\mathrm{ON},i}^{\mathrm{WRM}}(k)\leq 1;
\end{aligned}
\tag{26m}
$$

$$
\begin{aligned}
-\delta_i^{\mathrm{CLD}}(k-1)+\sigma_{\mathrm{CLD},i}^{\mathrm{STB}}(k)\leq 0,\\
-\delta_i^{\mathrm{STB}}(k)+\sigma_{\mathrm{CLD},i}^{\mathrm{STB}}(k)\leq 0,\\
\delta_i^{\mathrm{CLD}}(k-1)+\delta_i^{\mathrm{STB}}(k)-\sigma_{\mathrm{CLD},i}^{\mathrm{STB}}(k)\leq 1;
\end{aligned}
\tag{26n}
$$

$$
\begin{aligned}
-\delta_i^{\mathrm{STB}}(k-1)+\sigma_{\mathrm{STB},i}^{\mathrm{OFF}}(k)\leq 0,\\
-\delta_i^{\mathrm{OFF}}(k)+\sigma_{\mathrm{STB},i}^{\mathrm{OFF}}(k)\leq 0,\\
\delta_i^{\mathrm{STB}}(k-1)+\delta_i^{\mathrm{OFF}}(k)-\sigma_{\mathrm{STB},i}^{\mathrm{OFF}}(k)\leq 1;
\end{aligned}
\tag{26o}
$$

$$
\begin{aligned}
-\delta_i^{\mathrm{ON}}(k-1)+\sigma_{\mathrm{ON},i}^{\mathrm{OFF}}(k)\leq 0,\\
-\delta_i^{\mathrm{OFF}}(k)+\sigma_{\mathrm{ON},i}^{\mathrm{OFF}}(k)\leq 0,\\
\delta_i^{\mathrm{ON}}(k-1)+\delta_i^{\mathrm{OFF}}(k)-\sigma_{\mathrm{ON},i}^{\mathrm{OFF}}(k)\leq 1.
\end{aligned}
\tag{26p}
$$

where $\sigma_{\alpha_i}^{\beta} \in [0,1]$, and analogously to $\delta_i^{\alpha}(k)$s, they can only assume values $\{0,1\}$ due to (26).

A.3 Multi-objective proposed MPC formulation

The proposed control algorithm achieve its goal in two steps: the first consists in computing the optimal available power increment such that the weighted average of all increments within certain time windows is minimum. The second step minimize the mean square error between the available power downstream the hydrogen-based ESS and the grid operator reference using the previously computed optimal available power increment as a constraint. Thus, for a given

time instant k the first cost function is

$$J_{\mathrm{s}}(k) := \sum_{j=0}^{T-1} \sum_{\tau=1}^{\tau_B} \omega^{j,\tau} y^{k+j,\tau}, \tag{27}$$

for some control horizon T, τ_B previous samples and where $\omega^{j,\tau} \in (0,1)$ are some weights such that $\sum_{\tau=1}^{\tau_B} \omega^{j,\tau} = 1$ for each $j \in \{0,\dots,T-1\}$ and $y^{k+j,\tau}$ is the power increment between the available power at the time instant $k+j$ and the available power at τ steps back in the past (w.r.t. $k+j$).

Each $y^{k+j,\tau}$ is subject to the constraints

$$y^{k+j,\tau} \geq |P_{\mathrm{avl}}(k+j) - P_{\mathrm{avl}}(k+j-\tau)| - \bar{y}^{\tau}, \tag{28a}$$

$$y^{k+j,\tau} \geq 0, \tag{28b}$$

with $j \in \{0,\dots,T-1\}$, $\tau \in \{1,\dots,\tau_B\}$ and where $P_{\mathrm{avl}}(k+j)$ and $P_{\mathrm{avl}}(k+j-\tau)$ are the available powers at the time instant $k+j$ and at the time instant $k+j-\tau$, respectively, and $\bar{y}^{\tau}$ is a given power reference depending on τ.

Now, in order to set up the minimization problem in an MPC setting, we can cast (27) in vector form as

$$J_{\mathrm{s}}(k) = (\omega_k^{T-1})^{\top} y_k^{T-1} \tag{29}$$

with being $\omega_k^{T-1} := \mathrm{col}(\omega_k^{T-1,\tau})$ and $y_k^{T-1} := \mathrm{col}(y_k^{T-1,\tau})$,

$$\omega_k^{T-1,\tau} := \begin{pmatrix} \omega^{k,\tau} & \cdots & \omega^{k+T-1,\tau} \end{pmatrix}^{\top}, \tag{30a}$$

$$y_k^{T-1,\tau} := \begin{pmatrix} y^{k,\tau} & \cdots & y^{k+T-1,\tau} \end{pmatrix}^{\top}, \tag{30b}$$

where τ runs within the set $\{1,\dots,\tau_B\}$ and $\mathrm{col}(\cdot)$ is the column-wise stacking operator. Notice that $\mathrm{col}(\cdot)^{\top} = \mathrm{row}(\cdot^{\top})$, being $\mathrm{row}(\cdot)$ the row-wise stacking operator.

Similarly, let $P_{\mathrm{avl},k}^{T-1} := \mathrm{col}(P_{\mathrm{avl},k}^{T-1,\tau})$ where

$$P_{\mathrm{avl},k}^{T-1,\tau} := \left(\left| P_{\mathrm{avl}}(k) - P_{\mathrm{avl}}(k-\tau) \right| \cdots \left| P_{\mathrm{avl}}(k+T-1) - P_{\mathrm{avl}}(k+T-1-\tau) \right| \right)^{\top}, \tag{31}$$

and let A be a matrix with τ_B rows and $T\tau_B$ columns defined as

$$A := \begin{pmatrix} \mathbf{1}^{1\times T} & 0 & \cdots & 0 \\ 0 & \ddots & \ddots & 0 \\ \vdots & \ddots & \ddots & \vdots \\ 0 & \cdots & 0 & \mathbf{1}^{1\times T} \end{pmatrix}, \tag{32}$$

where $\mathbf{1}^{1\times T} := \begin{pmatrix} 1 & \cdots & 1 \end{pmatrix}$ has T columns.

Let us now introduce the set $\mathscr{C}$ of all the decision variable vectors defined as

$$\mathscr{C}_k := \{ y_k^{T-1}, P_{\mathrm{i},k}^{T-1}, P_{\mathrm{avl},k}^{T-1}, \delta_{\mathrm{i},k}^{\alpha,T-1}, \sigma_{\alpha,\mathrm{i},k}^{\beta,T-1}, z_{\mathrm{i},k}^{\gamma,T-1} \}, \tag{33}$$

where y_k^{T-1} is given in (30b) and

$$P_{\mathrm{i},k}^{T-1} := \Big(P_{\mathrm{i}}(k) \cdot \cdots \cdot P_{\mathrm{i}}(k+T-1)\Big)^{\top}, \tag{34a}$$

$$P_{\mathrm{avl},k}^{T-1} := \Big(P_{\mathrm{avl},i}(k) \cdot \cdots \cdot P_{\mathrm{avl}}(k+T-1)\Big)^{\top}, \tag{34b}$$

$$\delta_{\mathrm{i},k}^{\alpha,T-1} := \Big(\delta_{\mathrm{i}}^{\alpha}(k) \cdot \cdots \cdot \delta_{\mathrm{i}}^{\alpha}(k+T-1)\Big)^{\top}, \tag{34c}$$

$$\sigma_{\alpha,\mathrm{i},k}^{\beta,T-1} := \Big(\sigma_{\alpha,\mathrm{i}}^{\beta}(k) \cdot \cdots \cdot \sigma_{\alpha,\mathrm{i}}^{\beta}(k+T-1)\Big)^{\top}, \tag{34d}$$

$$z_{\mathrm{i},k}^{\gamma,T-1} := \Big(z_{\mathrm{i}}^{\gamma}(k) \cdot \cdots \cdot z_{\mathrm{i}}^{\gamma}(k+T-1)\Big)^{\top}, \tag{34e}$$

with being $i \in \{\mathrm{e},\mathrm{f}\}$, $\alpha,\beta \in \{\mathrm{OFF},\mathrm{CLD},\mathrm{STB},\mathrm{WRM},\mathrm{ON}\}$, $\alpha \neq \beta$ and $\gamma \in \{\geq 0, \leq 0, \geq P_i^{\mathrm{CLD}}, \leq P_i^{\mathrm{CLD}}, \geq P_i^{\mathrm{STB}}, \leq P_i^{\mathrm{STB}}, \geq P_i^{\mathrm{WRM}}, \leq P_i^{\mathrm{WRM}}, \geq P_i^{\mathrm{min}}, \leq P_i^{\mathrm{max}}\}$.

Therefore, the problem of minimizing (29) subject to (28), can be stated as

$$\begin{aligned} \min_{\mathscr{C}_k} \quad & J_{\mathrm{s}}(k) \\ \text{s.t.} \quad & y_k^{T-1} \geq 0, \\ & A y_k^{T-1} \geq A P_{\mathrm{avl},k}^{T-1} - \mathbf{1}^{T\tau_B \times 1} \bar{y}^{\tau}, \\ & (22)-(24), \\ & (26)-(14), \\ & \text{box and logic constraints for } \delta_i^{\alpha}(k)\text{s, } \sigma_{\alpha,i}^{\beta}(k)\text{s and } z_i^{\gamma}(k)\text{s}, \end{aligned} \tag{35}$$

where $\mathscr{C}_k$ is given in (33), $\mathbf{1}^{T\tau_B \times 1} := \Big(1 \cdot \cdots \cdot 1\Big)^{\top}$ has $T\tau_B$ rows, $\delta_i^{\alpha}(k), \sigma_{\alpha,i}^{\beta}(k) \in [0,1]$ and $z_i^{\gamma}(k) \in \{0,1\}$, for each $i \in \{\mathrm{e},\mathrm{f}\}$, with $\alpha,\beta \in \{\mathrm{OFF},\mathrm{CLD},\mathrm{STB},\mathrm{WRM},\mathrm{ON}\}$, $\alpha \neq \beta$ and $\gamma \in \{\geq 0, \leq 0, \geq P_i^{\mathrm{CLD}}, \leq P_i^{\mathrm{CLD}}, \geq P_i^{\mathrm{STB}}, \leq P_i^{\mathrm{STB}}, \geq P_i^{\mathrm{WRM}}, \leq P_i^{\mathrm{WRM}}, \geq P_i^{\mathrm{min}}, \leq P_i^{\mathrm{max}}\}$.

Now, we are ready to introduce the second step where the tracking error is minimized. Accordingly, the proposed cost function for a given time instant k is

$$J_{\mathrm{l}}(k) := \frac{1}{T} \sum_{j=0}^{T-1} \Big(P_{\mathrm{avl}}(k+j) - P_{\mathrm{ref}}(k+j)\Big)^2, \tag{36}$$

where T is the control horizon.

Then, the optimal value J_{s}^* attained in (35) is included as a constraint within the minimization step of (36) in order to consequently bound the available power P_{avl}, therefore resulting in:

$$\begin{aligned} \min_{\mathscr{C}_k} \quad & J_{\mathrm{l}}(k) \\ \text{s.t.} \quad & A P_{\mathrm{avl},k}^{T-1} \leq \mathbf{1}^{T\tau_B \times 1} \bar{y}^{\tau} + A y_k^{T-1}, \\ & y_k^{T-1} \geq 0, \\ & (\omega_k^{T-1})^{\top} y_k^{T-1} \leq J_{\mathrm{s}}^*, \\ & (22)-(24), \\ & (26)-(14), \\ & \text{box and logic constraints for } \delta_i^{\alpha}(k)\text{s, } \sigma_{\alpha,i}^{\beta}(k)\text{s and } z_i^{\gamma}(k)\text{s}. \end{aligned} \tag{37}$$

References

[1] "Hydrogen-aeolic energy with optimized electrolysers upstream of substation project," http://www.haeolus.eu/.

[2] A. Hoskin, A. S. Pedersen, E. Varkaraki, F. J. Pino, I. Aso, J. Simón, J. Lehmann, J. Linnemann, K. Stolzenburg, L. Castrillo, M. Rey, P. Fontela, R. Garde, R. Schmid, R. Mubbala, R. Gammon, S. Suarez, S. T. Briskeby, and S. Nygaard, "Task 24: Wind energy and hydrogen integration—final report," International Energy Agengy – Hydrogen Implementing Agreement, Tech. Rep., 2013. [Online]. Available: http://ieahia.org/pdfs/Task_24_final_report.aspx

[3] L. Meng, T. Dragicevic, and J. M. Guerrero, "Adaptive control design for autonomous operation of multiple energy storage systems in power smoothing applications," *IEEE Transactions on Industrial Electronics*, vol. 65, no. 8, pp. 6612–6624, Aug 2018.

[4] A. Bemporad and M. Morari, "Control of systems integrating logic, dynamics, and constraints," *Automatica*, vol. 35, no. 3, pp. 407–427, 1999.